ELSEVIER

Thermochimica Acta 295 (1997) 59–71

thermochimica acta

Influence of mass transfer on interaction between thermoanalytical and mass spectrometric curves measured in combined thermoanalyser–mass spectrometer systems

B. Roduit[a], J. Baldyga[b], M. Maciejewski[a], A. Baiker[a,*]

[a]*Department of Chemical Engineering and Industrial Chemistry, Swiss Federal Institute of Technology, ETH-Zentrum, CH-8092 Zurich, Switzerland*

[b]*Department of Chemical and Process Engineering, Warsaw University of Technology, PL-00-645 Warsaw, Poland*

Abstract

The convective and diffusional mass transfer occurring in combined thermoanalyser–mass spectrometer systems can cause significant deviation between measured thermoanalytical and mass spectrometric curves. Based on experimental studies of the decomposition of $CaCO_3$, a model has been developed which allows to interrelate the thermoanalytical (DTG) and mass spectrometric curves and provides a criterion defining under which conditions (carrier gas-flow rate and diffusivity of evolved gas) the disguising mass-transfer influences can be neglected. The criterion relates the total residence time τ_{tot} of the gas in the experimental system to the characteristic time t_N of the gravimetrically recorded decomposition process and allows to quantify the agreement between the thermoanalytical and mass spectrometric curves. © 1997 Elsevier Science B.V.

Keywords: Thermal analysis coupled with mass spectrometry; Influence of mass transfer on TA–MS signals

1. Introduction

Measurements of thermal decomposition of solids resulting in gaseous products are usually interpreted assuming that at any time the measured product concentration in the gaseous mixture leaving the thermoanalyser chamber characterises the rate of the reactant decomposition at that time. In reality, a time lag is observed between the DTG signal due to the decomposition and the mass spectrometric analysis of the evolving gaseous product. Moreover, the process of back-mixing in the thermoanalyser chamber can notably influence the shape of the concentration–response curve. Here, we illustrate how the mass spectrometrically measured concentration of a gaseous product can be related to the gravimetrically determined rate of the decomposition. In principle, a prediction of this relationship is only possible when the complete flow patterns (velocity distribution) in the thermoanalyser are known, which is very difficult to achieve in practice. One possibility to measure the flow pattern in the thermoanalyser is to scale-up the system and measuring the flow characteristics with Laser Doppler anemometry. Another approach is to solve the complex set of differential balance equations (Navier Stokes, species balances) for the complicated geometry of the thermoanalyser. Both methods are too demanding for practical purposes. A more straightforward approach is presented in this study, where the above relationship is analysed by a simple identification of the system which directly relates an input signal (decomposition) to the corresponding output signal (concentration of a gaseous product measured

*Corresponding author. E-mail: baiker@tech.chem.ethz.ch, fax: (+41-1) 632 11 63.

PII S0040-6031(97)00101-9

by the mass spectrometer (MS)). The function containing this information is the residence time distribution (RTD) of the system. The RTD function describes systems only in the time space (Lagrangian frame) and contains the minimum of information necessary to transform the input signal (stimulus) into the output signal (response). The stimulus–response technique in the system thermoanalyser–mass spectrometer is illustrated in Fig. 1.

Considering the system characterised by the residence-time–distribution-density function $f(t)$, the strict relationship between an arbitrary input and its output concentration can be expressed according to the set of equations (Eqs. (1a)–(1c) and (2b)), if the system is initially relaxed, i.e. $C_{in}(t) = 0$ for all $t < 0$.

$$C_{out}(t) = \int_0^t C_{in}(t - t')f(t')\,dt' \tag{1a}$$

$$= \int_0^t C_{in}(t')f(t - t')\,dt' \tag{1b}$$

or, after normalisation of stimulus and response

$$h(t) = \int_0^t g(t')f(t - t')\,dt' \tag{1c}$$

where

$$h(t) = \frac{C_{out}(t)}{\int_0^\infty C_{out}(t)\,dt} \tag{2a}$$

$$g(t) = \frac{C_{in}(t)}{\int_0^\infty C_{in}(t)\,dt} \tag{2b}$$

The identification of the residence-time–distribution-density function $f(t)$ appearing in Eqs. (1a)–(1c) is extracted from the experimental data. This function is then applied to the calculation of the concentration profiles measured by the mass spectrometer. Here, we use this concept to elucidate the relationship between thermoanalytical and mass spectrometric curves measured in combined thermoanalyser–mass spectrometer systems.

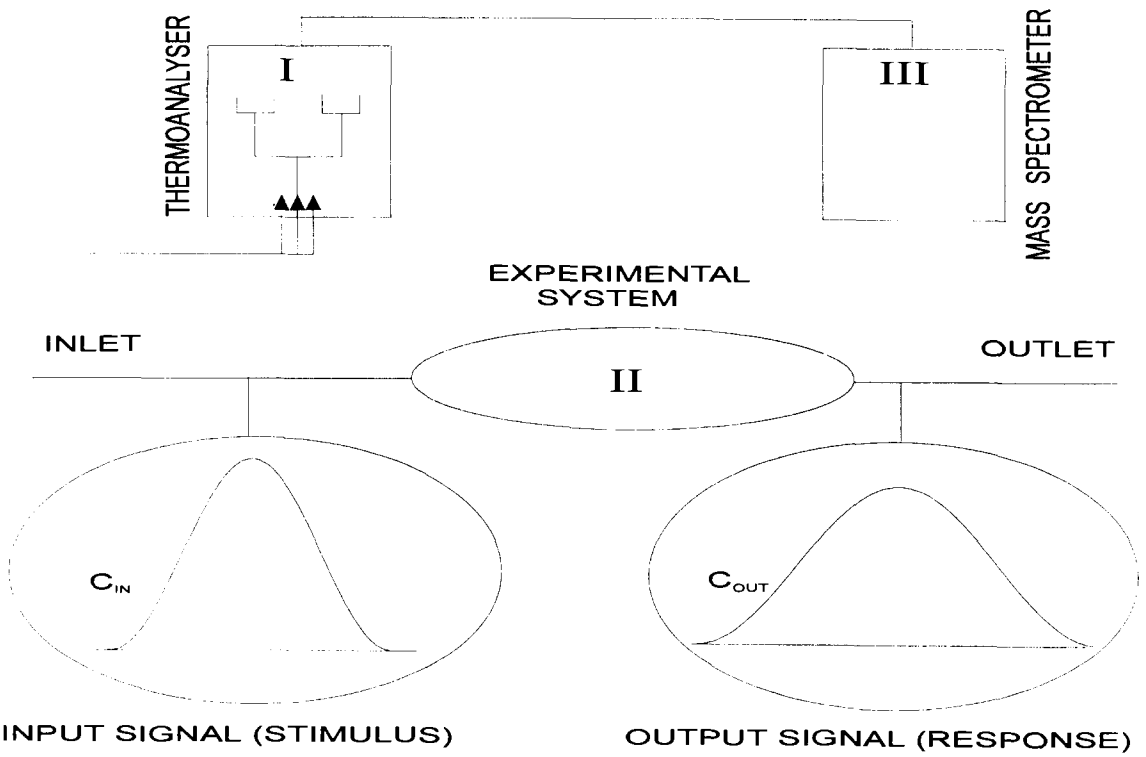

Fig. 1. Stimulus–response technique for a simple flow system. (I) Input signal detection; (II) experimental system; and (III) output signal detection.

2. Experimental and methods of calculation

The measurements were carried out on a Netzsch STA 409 thermoanalyser connected with Balzers QMG 420 mass spectrometer by a 0.15 mm heated capillary. As an input signal, the rate of CO_2 evolution resulting from the decomposition of 15.0 mg of $CaCO_3$ was applied. Experiments were carried out under argon atmosphere with flow rates of carrier gas ranging 20–100 ml min^{-1} (NTP) and using a heating rate of $\beta = 11.7$ K min^{-1}. The diameter and the height of the thermoanalyser chamber were 2.6 and 23 cm, respectively. The thermogravimetric curve reflects the release of CO_2 (input signal) to the stream of argon flowing through the experimental system. The stimulus can thus be calculated as the normalised rate of weight loss of the $CaCO_3$ (derivative thermogravimetric curve, DTG), and the rate of CO_2 production is directly related to the rate of weight loss of $CaCO_3$.

$$R(t) = -\frac{\mathrm{d(TG)}}{\mathrm{d}t} \tag{3}$$

After normalisation (compare with Eq. (2b))

$$g(t) = \frac{R(t)}{Q} \tag{4}$$

where Q is the whole amount of CO_2 produced during decomposition.

$$Q = \int_0^\infty R(t)\,\mathrm{d}t \tag{5}$$

The thermobalance system measures the weight losses of the sample ($CaCO_3$) during small and equal periods of time Δt. Eqs. (3)–(5) should thus be used in the discrete form. For the discrete t values, we can write

$$t = t_i = i\,\Delta t \tag{6}$$

$$R(t) = R(t_i) = R(i\,\Delta t) = -\frac{\mathrm{TG}(t_{i+1}) - \mathrm{TG}(t_i)}{t_{i+1} - t_i} = -\frac{\Delta i(\mathrm{TG})}{\Delta t} \tag{7}$$

$$Q = \sum_{i=1}^{\infty} -\frac{\Delta i(\mathrm{TG})}{\Delta t}\Delta t = -\sum_{i=1}^{\infty} \Delta i(\mathrm{TG}) \tag{8}$$

$$g(t) = g(t_i) = g_i = \frac{R(i\,\Delta t)}{Q} \tag{9}$$

Similarly, the response $h(t)$ is the normalised concentration of CO_2 measured by the mass spectrometer.

We have

$$h(t) = \frac{I(t)}{J} \tag{10}$$

$$J = \int_0^\infty I(t)\,\mathrm{d}t \tag{11}$$

$$J = \sum_{i=1}^{\infty} I(t_i)\,\Delta t = \sum_{i=1}^{\infty} I(i\,\Delta t)\,\Delta t \tag{12}$$

$$h(t) = h(t_i) = h_i = \frac{I(i\,\Delta t)}{J} \tag{13}$$

A typical record of the input signal $g(t)$ and the output signal $h(t)$ measured in the experimental system is shown in Fig. 2 for a total gas-flow rate of 40 ml min^{-1} (NTP). The curves have slightly different shapes. The method of calculation of the mutual relationship between the stimulus $g(t)$ and the response functions $h(t)$ is presented below.

3. Model

The model should allow a simple and clear interpretation of the difference between the $g(t)$ and $h(t)$

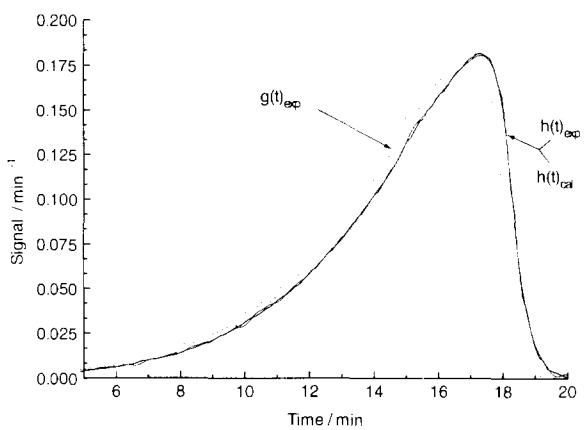

Fig. 2. Comparison between measured and calculated (mixed and plug flow model) responses $h(t)_{exp,\,cal}$ (MS-curve) for a given input signal $g(t)_{exp}$ (DTG). Total gas-flow rate: 40 ml min^{-1} (NTP).

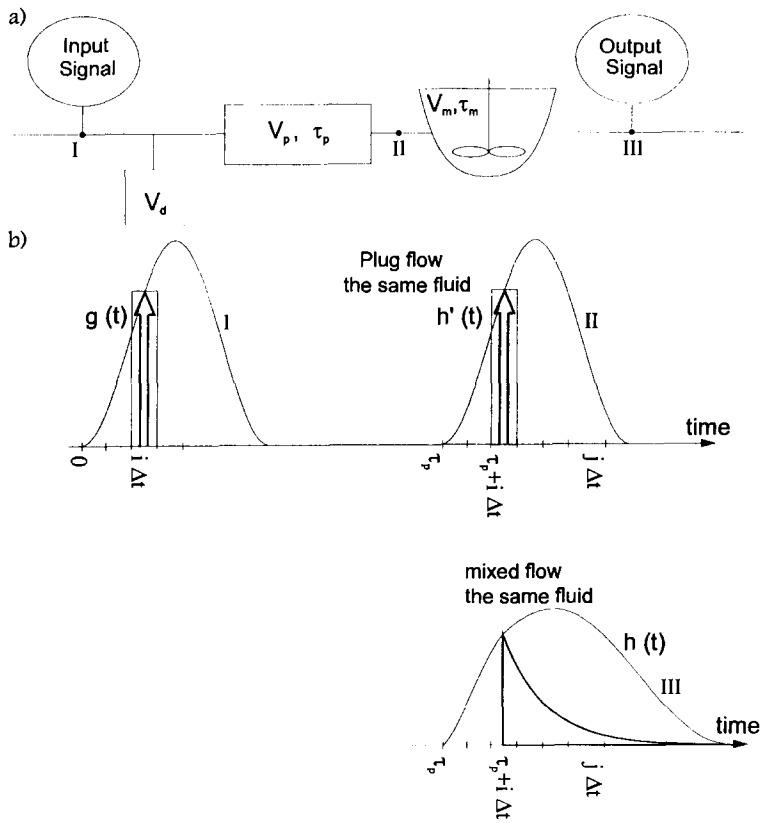

Fig. 3. (a) Simple flow model. (b) Scheme illustrating mixing of an elementary pulse in the system. Curves marked by I, II and III represent the signal measured at points I, II and III. Curves $g(t)$ and $h'(t)$ are identical, $h'(t)$ is only shifted due to the time lag τ_p. We denote by $g(t)$: the normalised input signal given by the thermoanalyser; $h'(t)$: the normalised input signal given by the thermoanalyser after the plug flow zone ($h'(t) = g(t-\tau_p)$); $h(t)$: the normalised output signal given by the mass spectrometer; τ_p and τ_m: the residence times in the plug and mixed flow zone, respectively. V_d, V_p and V_m: the volumes of the dead, plug and mixed-flow zone, respectively.

curves. We can distinguish three zones [1] in the thermobalance chamber, which differ concerning the governing mass-transfer conditions:

1. the plug-flow or piston-flow zone, where the input signal is delayed;
2. the mixed-flow zone, where the input signal changes its shape due to back-mixing; and
3. the dead-fluid zone, where CO_2 produced in the decomposition process does not enter.

The simplest model having all required features is shown schematically in Fig. 3a. For this system, the volumes of the plug and the mixed-flow zones, V_p and V_m, respectively, are calculated. The rest of the chamber volume forms the dead-fluid zone, which represents the zone into which CO_2 does not enter. This zone can be calculated, but does not influence directly the CO_2 profile. The input signal is considered to be a set of idealised pulses (Dirac delta functions) injected into the system with a frequency $\nu = 1/\Delta t$ and equal to $\Delta t g(i\,\Delta t)\,\delta(t - i\,\Delta t)$.

A scheme showing the mixing steps of a pulse in the system is presented in Fig. 3b.

We have

$$h'(t_i) = \begin{cases} 0 & \text{for} \quad t_i < \tau_p \\ g(t_i - \tau_p) & \text{for} \quad t_i \geq \tau_p \end{cases} \tag{14}$$

or in a discrete form

$$h'(t_i) = \begin{cases} 0 & \text{for} \quad i\,\Delta t < \tau_p \\ g(i\,\Delta t - \tau_p) & \text{for} \quad i\,\Delta t \geq \tau_p \end{cases} \tag{15}$$

In the well-mixed zone of the system, the mean of the residence time is τ_m and the residence-time distribution can be expressed as:

$$f'(t) = \frac{1}{\tau_m} \exp\left(-\frac{t}{\tau_m}\right) \tag{16}$$

The response to each pulse $\Delta t\, g(t_i)\,\delta(t - t_i)$ entering the well-mixed zone at $t = t_i$ should be thus

$$h(t_i,\ t_j - t_i) = \Delta t\, g(t_i - \tau_p)\frac{1}{\tau_m}\exp\left(-\frac{t_j - t_i}{\tau_m}\right) \tag{17}$$

when observed at $t = t_j$ $(j > i)$. The responses of all signals entering the well-mixed zone before $t = t_j$ can overlap. Thus, the observed response in the mixed zone equals the sum of all of them:

$$h(t_j) = \frac{\Delta t}{\tau_m}\sum_{i=\frac{\tau_p}{\Delta t}}^{j} g(t_i - \tau_p)\exp\left(-\frac{t_j - t_i}{\tau_m}\right) \tag{18}$$

or

$$h(t_j) = h(j\,\Delta t) = \frac{\Delta t}{\tau_m}\sum_{i=\frac{\tau_p}{\Delta t}}^{j} g(i\,\Delta t - \tau_p)\exp\left(-\frac{(j-i)\Delta t}{\tau_m}\right) \tag{19}$$

This procedure is equivalent to using Eq. (1c) with the presumed form of the residence time-distribution function.

4. Results and discussion

4.1. Calculation of the output signal $h(t)_{cal}$ (MS curve) from known τ_p and τ_m and measured input signal $g(t)_{exp}$ (DTG)

The flow model and the $h(t_j)$ calculated from the experimental input signal are functions of the two parameters τ_p and τ_m. The values of τ_p and τ_m can be calculated as related to the minimum of the total residual sum of squares of the difference between the experimental and calculated values of $h(t_j)$.

Objective function : $\mathrm{RSS}(\tau_p,\ \tau_m)$

$$= \sum_{i=0}^{\infty}[h_{exp}(t_i) - h_{cal}(t_i;\ \tau_p,\ \tau_m)]^2 \tag{20}$$

The comparison between measured and calculated (mixed- and plug-flow models) responses $h(t)_{exp,\ cal}$ (MS curve) for a given input signal $g(t)_{exp}$ (DTG curve) is shown in Fig. 2 for the carrier gas-flow rate of 40 ml min^{-1}.

Similar fittings and recalculations were performed for other flow rates of argon. The results are shown in Fig. 4.

We can evaluate the accuracy of our model by comparing the volume of the thermoanalytical chamber to the values calculated from the total residence times needed in both plug and mixed-flow reactors.

The volume of the thermoanalytical chamber is:

$$V_{exp} = H\pi(D/2)^2 = 23\pi(2.6/2)^2\ \mathrm{cm} \times \mathrm{cm}^2 \cong 122\ \mathrm{cm}^3 \tag{21}$$

We have

$$V_{cal} = V_p + V_m = F_0\frac{\bar{T}}{T_0}\frac{P_0}{P}(\tau_p + \tau_m) \tag{22}$$

with $P_0 = 1$ atm, $T_0 = 298$ K, $P = 1$ atm, $\bar{T} = (273+730) = 1003$ K (where 730°C represents the average temperature for 50% conversion of $CaCO_3$ for the five considered gas-flow rates F_0: 20, 40, 50, 80 and 100 ml min^{-1} (NTP)).

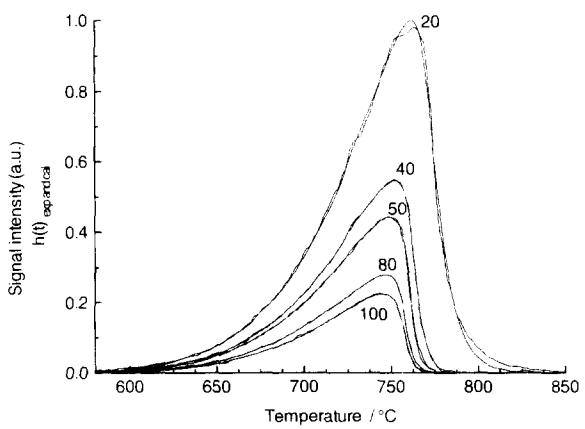

Fig. 4. Intensity of the output signal as a function of the gas flow rate. On the presented curves, the total gas-flow rate is expressed in ml min^{-1} (NTP).

Table 1
Volumes and residence times as function of the total gas-flow rate

F_0	ml min^{-1}	20	40	50	80	100
τ_p	min	0.326	0.189	0.185	0.183	0.175
V_p	ml	21.94	25.45	31.13	49.27	58.90
τ_m	min	0.684	0.305	0.186	0.084	0.041
V_m	ml	46.04	41.06	31.30	22.62	13.80
$\tau_{tot} = \tau_p + \tau_m$	min	1.01	0.49	0.37	0.27	0.22
$V_{cal} = V_{tot} = V_p + V_m$	ml	67.99	66.51	62.44	71.89	72.70
$L_{cal} = V_{cal}/(\pi(D/2)^2)$	cm	12.81	12.53	11.76	13.54	13.69
$V_d = V_{exp} - V_{cal}$	ml	54.01	55.49	59.56	50.11	49.30
RSS	min^{-2}	1.02*E*−3	1.95*E*−4	3.61*E*−4	2.41*E*−4	6.81*E*−4

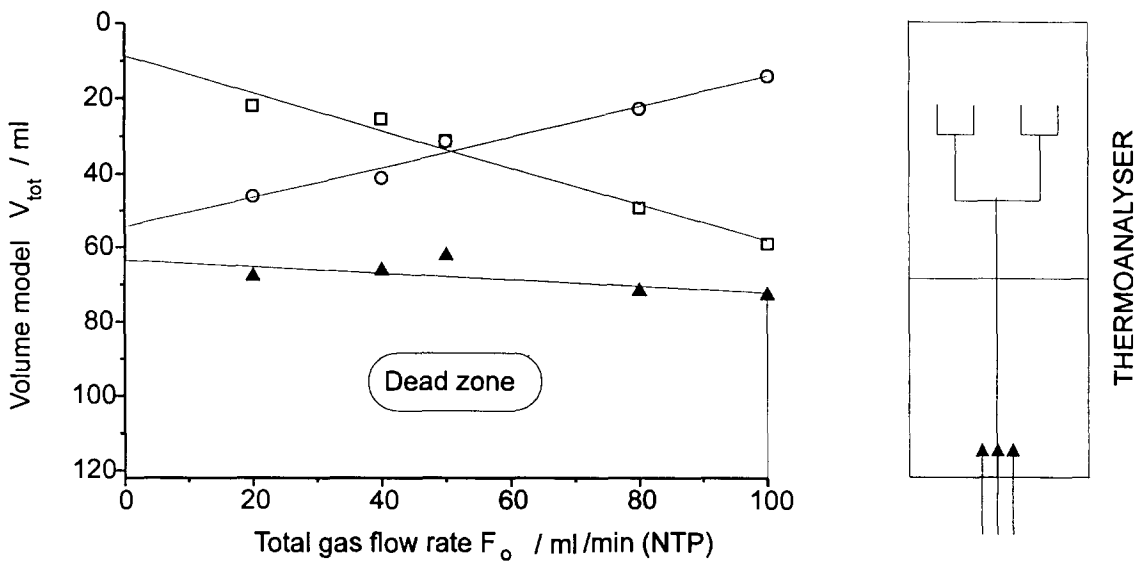

Fig. 5. Dependence of the V_p and V_m volume on the total gas-flow rate. Total calculated volume $V_{cal} = V_p + V_m$ (▲). Calculated mixed-flow volume V_m (○). Calculated plug-flow volume V_p (□). The shaded area represents the dead zone in which the gas evolved by decomposition does not enter.

The results of the calculations are listed in Table 1 and the general dependencies of the V_p and V_m volumes on the flow rate are illustrated in Fig. 5. The dead volume can also be estimated from the difference between the experimental and calculated volumes. Applying our model, we can calculate the time lag τ_p and determine the slight or significant shift in the output signal. Regarding the influence of the residence time τ_m, we obtain an indication concerning the deformation of the shape of the input signal. An increase in the total gas-flow rate reduces the mixed-flow volume V_m and increases the plug-flow volume (Table 1 and Fig. 5). An increase in the total gas-flow rate reduces both residence times τ_p and τ_m, because the total volume V_{cal} remains unchanged as emerges from Fig. 5.

4.2. *Calculation of input function $g(t)_{cal}$ (DTG) from known τ_p and τ_m and measured output function $h(t)_{exp}$ (MS curve)*

This procedure allows us to calculate the input signal originating from the release of CO_2 during $CaCO_3$ decomposition (DTG) from the recorded

MS signal. We can distinguish between the contributions from plug- and mixed-flow to the system and treat them separately.

4.2.1. Influence of plug flow

For the calculation, the influence of the plug flow is eliminated by shifting the output function $h(t)$ by τ_p to the left:

$$h''(t) = h(t + \tau_p) \tag{23}$$

or in a discrete form

$$h''(t_i) = h''(i\,\Delta t) = h(i\,\Delta t + \tau_p) \tag{24}$$

The sequence of ideal zones [1] representing our model does not influence the result. The scheme applied for the calculation of the input signal from the observed output signal is illustrated in Fig. 6.

4.2.2. Influence of mixed flow

The material balance gives:

$$g(t) = h''(t) + \frac{\mathrm{d}h''}{\mathrm{d}t}\tau_m \tag{25}$$

or in a discrete form

$$g(t_i) = g(i\,\Delta t) = h''(i\,\Delta t) + \frac{h''((i+1)\,\Delta t) - h''(i\,\Delta t)}{\Delta t}\,t_m \tag{26}$$

Knowing τ_m and $h''(t)$, the input signal $g(t)_{cal}$ can easily be calculated using Eq. (26). The comparison of experimental and calculated input signal (DTG) from measured MS curve is illustrated in Fig. 7. Similar calculations were performed for the other flow rates of argon: 20, 50, 80 and 100 ml min^{-1} (NTP), demonstrating the accuracy of the model.

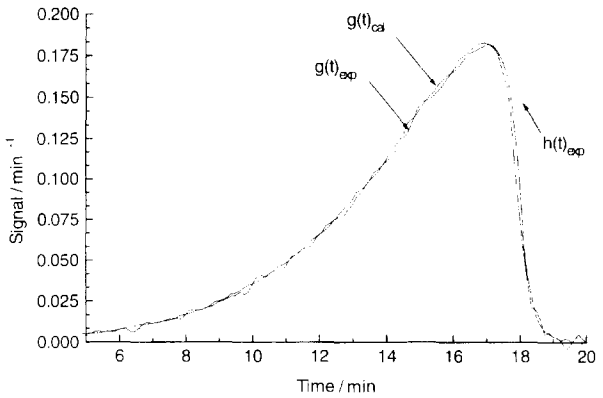

Fig. 7. Comparison of experimental and calculated input signal $g(t)_{exp.cal}$ (DTG) from measured $h(t)_{exp}$ (MS curve). Total gas-flow rate is 40 ml min^{-1} (NTP).

4.3. Influence of the diffusion of the evolved gas in the carrier gas

Regarding the behaviour of the response signal given by the mass spectrometer, we have observed that an increase in the flow rate of carrier gas increases the plug-flow region and significantly reduces the mixed-flow zone as emerges from Table 1. In order to check whether the considerations taking into account the molecular diffusion coefficient of CO_2

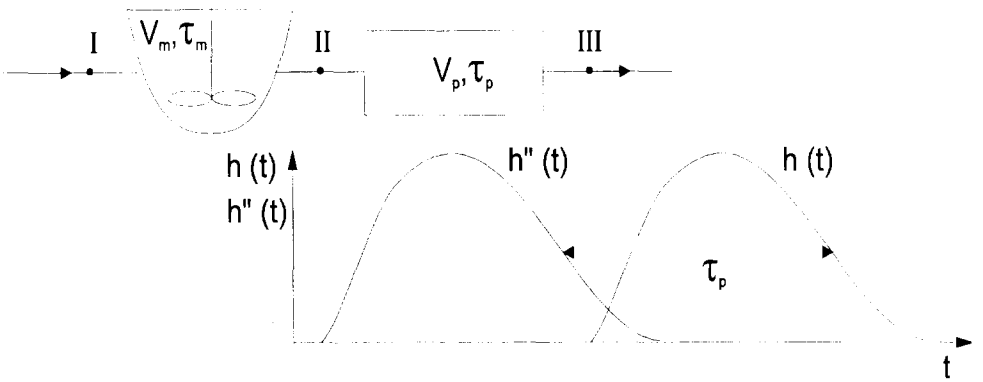

Fig. 6. Scheme for the calculation of the input signal $g(t)_{cal}$ from observed output signal $h(t)_{exp}$. The influence of the plug flow is removed by shifting the output function $h(t)_{exp}$ by τ_p to the left ($h''(t) = h(t + \tau_p)_{exp}$).

in argon lead to similar conclusions, the following calculations were performed. The molecular diffusion coefficient was calculated from the expression [2,3]:

$$D_{CO_2,\,Ar} = \frac{0.0018583\,T^{\frac{3}{2}}\left[(M_{CO_2}+M_{Ar})/(M_{CO_2}M_{Ar})\right]^{0.5}}{P\sigma^2_{CO_2,\,Ar}\,\Omega}$$

with

$$\Omega = f\left(\frac{kT}{\varepsilon_{CO_2,\,Ar}}\right) \tag{28}$$

$$\varepsilon_{CO_2,\,Ar} = \sqrt{\varepsilon_{CO_2}\,\varepsilon_{Ar}} \tag{29}$$

$$\sigma_{CO_2,\,Ar} = 0.5(\sigma_{CO_2} + \sigma_{Ar}) \tag{30}$$

and $M_{CO_2} = 44.01\ g\,mol^{-1}$, $M_{Ar} = 39.95\ g\,mol^{-1}$, $P = 1\times10^5$ Pa, $\sigma_{CO_2} = 3.941$ A, $\sigma_{Ar} = 3.542$ A, $\varepsilon_{CO_2}/k = 195.2$ K, $\varepsilon_{Ar}/k = 93.3$ K, $\Omega = f(7.43) \cong 0.78$, we obtain at $\bar{T} = 1003$ K, $D_{CO_2,\,Ar} = 1.17\ cm^2\,s^{-1}$.

Considering the relationship between the diffusion path length and the residence time (also diffusion time) in a pipe (well-mixed and plug-flow zone),

$$\tau_{tot} = \frac{L_D^2}{D_{CO_2,\,Ar}} \tag{31}$$

where L_D represents the length of the thermoanalytical chamber over which diffusion occurs, we obtain after rearranging Eq. (31):

$$L_D = \sqrt{D_{CO_2,\,Ar}\,\tau_{tot}} \tag{32}$$

which leads to the ratio L_D/L_{cal}, where $L_{cal} = V_{cal}/(\pi(D/2)^2)$ characterises the length of the thermoanalytical chamber without the dead zone. The values of L_D/L_{cal} are summarised in Table 2.

As emerges from Table 2, an increase in the gas-flow rate leads to a significant decrease in the ratio L_D/L_{cal}. The total volume V_{cal}, remaining unchanged upon increasing the total gas-flow rate, indicates that the importance of the plug-flow zone significantly grows when the mixed-flow zone decreases and vice versa.

4.4. Determination of the minimal total gas-flow rate above which no significant difference between input (DTG) and output signal (MS curve) can be observed

If the residence time in the plug-flow region is infinitely short, the curves $g(t)$ and $h(t)$ will depend only on the mixing zone and the influence of the residence time in the plug-flow region, expressed by a time lag of the output signal, is negligible. Using the statistic F-test, we can introduce the ratio τ_{tot}/t_N as a criterion which relates the effects of progress of solid decomposition, rate of mass transfer by convection, diffusion or dispersion and total gas-flow rate. In this criterion, t_N is the characteristic time of the decomposition process, defined as:

$$t_N = \frac{|\Delta g|}{|\partial g/\partial t|_{max}} \tag{33}$$

The subscript 'max' indicates that the maximal rate of the change of the input signal 'g' is considered. The graphical determination of t_N is presented in Fig. 8. With the given criterion, we can determine whether the influence of the gas flow on the output signal is negligible or significant from a statistical point of view. The F-distribution function is used for calculating the 95% confidence limit for the minimum gas-flow rate required for a proper description of the thermoanalytical curve from the measured MS curve. Under these conditions, the deviation of two repeated measurements equals that between the input and the

Table 2
The ratio L_D/L_{cal} as a function of the total gas-flow rate assuming constant total volume V_{cal} (see Table 1 and Fig. 5)

F_0(NTP)	ml min^{-1}	20	40	50	80	100
τ_{tot}	min	1.01	0.49	0.37	0.27	0.22
L_D	cm	8.42	5.89	5.10	4.33	3.89
L_{cal}	cm	12.81	12.53	11.76	13.54	13.69
L_D/L_{cal}	%	66	47	43	32	28

L_D: length of the thermoanalytical chamber over which diffusion occurs. L_{cal}: calculated length of the thermoanalytical chamber without the dead zone.

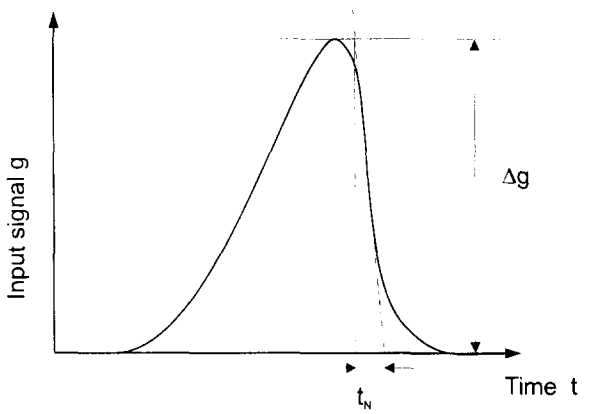

Fig. 8. Graphical presentation of the characteristic time of the decomposition process t_N expressed as $t_N = |\Delta g|/|\partial g/\partial t|_{max}$, where subscripts 'max' indicates the maximal rate of the change of the input signal g.

output signal, as explicitly shown in Eqs. (37) and (38). In such a situation, an increase in the gas flow is not required any more because, from a statistical point of view, it will not improve the accuracy of the description of the DTG curve by the MS curve, and from the experimental side, it decreases the sensitivity of the analysis.

4.5. Determination of the F-distribution

To perform the F-test for the chosen confidence level, the F-distribution can be approximated with Eq. (34)[4] if $f_1 > 4$ and $f_2 > 5$

$$F(f_1 \approx 150,\ f_2 \approx 150,\ P = 0.95) = e^{2z(f_1, f_2, P)} \tag{34}$$

where:

f_j	degrees of freedom of the F-distribution, equal to the number of experimental points n;
subscript '1'	repeated experimental conditions in order to consider the experimental error;
subscript '2'	input and output signals;
n	number of the experimental points for one signal ($\sim$ 150); and
P	probability: 95%.

z in Eq. (34) is expressed by the formula:

$$\begin{aligned} z(f_1, f_2, P) = {} & \frac{u_P}{\sqrt{h}} - \frac{d}{6}(u_P^2 + 2) \\ & + \frac{1}{\sqrt{h}}\left[\frac{u_P^3 + 3u_P}{12h} + \frac{(u_P^3 + 11u_P)hd^2}{144}\right] \\ & - \frac{d}{60h}(u_P^4 + 9u_P^2 + 8) \\ & + \frac{hd^3}{6480}(3u_P^4 + 7u_P^2 - 16) \\ & + \frac{1}{h}\left[\frac{u_P^5 + 20u_P^3 + 15u_P}{480h^2} + \frac{(u_P^5 + 44u_P^3 + 183u_P)d^4}{2880}\right] \\ & + \frac{d^4h^2}{622080}(9u_P^5 - 284u_P^3 - 1513u_P) \end{aligned}$$

where

$$d = \frac{1}{f_1} - \frac{1}{f_2} \text{ and } h = \frac{2}{\frac{1}{f_1} + \frac{1}{f_2}}$$

The value of the standard normal distribution u_P for $P = 95\%$ and $f_1 \approx 150$ and $f_2 \approx 150$ is equal to 1.6759.

In order to compare quantitatively the similarity of the experimental data given by the mass spectrometer (output signal) and the thermoanalyser (input signal), and the data obtained from the thermoanalyser during two repeated identical conditions (input signal), we applied the following expression:

$$F_{exp} = \frac{RSS_2/f_2}{RSS_1/f_1} \tag{36}$$

with $RSS_1/f_1 > RSS_2/f_2$, where RSS_1/f_1 is the sum of residual squares between two (in order to consider the influence of the experimental errors) experiments performed under the same conditions and RSS_2/f_2 is the sum of residual squares for one flow rate between the input and output signals given by the thermoanalyser and the mass spectrometer, respectively.

RSS is defined as follows:

$$RSS_1 = \sum_{i=1}^{n}(\text{input signal}_i - \text{input signal}_{\text{repeated},\,i})^2 \tag{37}$$

$$RSS_2 = \sum_{i=1}^{n}(\text{input signal}_i - \text{output signal}_i)^2 \tag{38}$$

Table 3
Ratios τ_{tot}/t_N and F_{exp}/F as functions of the total gas-flow rate F_0 and $1/\tau_{tot}$. ($F_0 \propto 1/\tau_{tot}$ because $V_{cal} \cong$ constant Eq. (22))

F_0	cm^3 min(NTP)	20	40	50	80	100
$1/\tau_{tot}$	min^{-1}	0.99	2.04	2.70	3.70	4.54
τ_{tot}/t_N	—	1.09	0.77	0.60	0.44	0.32
F_{exp}/F	—	8.07	3.41	1.75	0.83	0.57

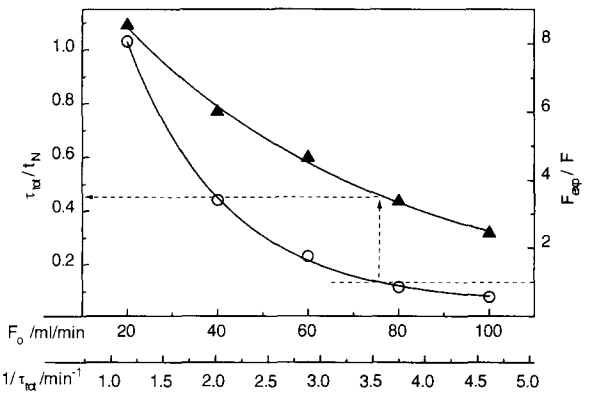

Fig. 9. Ratios τ_{tot}/t_N (△) and F_{exp}/F (○) as functions of the total gas-flow rate F_0 and $1/\tau_{tot}$. A ratio F_{exp}/F greater than 1 indicates that for flow rates lower than about 75 ml min^{-1} or for ratio τ_{tot}/t_N higher than 0.45, the output signal does not describe properly the input signal given by the thermoanalyser.

A ratio $F_{exp}/F > 1$ indicates that the output signal determined for the considered flow rate does not describe properly the input signal given by the thermoanalyser.

By repeating the F-test for all flow rates 20, 40, 50, 80 and 100 ml min^{-1} (NTP) (Table 3 and Fig. 9), we find that for flow rates higher than ~ 75 ml min^{-1} (NTP), no significant difference between the input and its corresponding output signal is observable ($F_{exp}/F \leq 1$). Thus the criterion τ_{tot}/t_N allows to quantify the influence of the gas-flow rate on the proper description of the input signal (DTG) by the output signal (MS).

According to Fig. 9 and Table 3, for a ratio $\tau_{tot}/t_N < 0.45$, the difference between the input and output signal is negligible. The choice of the carrier gas influences this critical value.

When the diffusivity of evolved gas (in our case CO_2) is higher in another carrier gas, then an increase in the total flow is required to fulfil the global criterion of the residence time. For another carrier gas, the diffusion path length L_D can be set as equal to that in Ar in order to keep the same relation between the DTG and MS curves:

$$L_{D,\,Ar,\,crt} = L_{D,\,NC,\,crt} \tag{39}$$

where NC is new carrier gas under which the decomposition occurs and 'crt' is critical value given by the criterion of the residence time, with

$$L_{D,\,NC,\,crt} = \sqrt{D_{CO_2,\,NC}\,\tau_{tot,\,crt}} = \sqrt{D_{CO_2,\,NC}\,\frac{L_{cal,\,crt}}{\bar{u}_{NC,\,crt}}} \tag{40}$$

and the expression of the gas velocity

$$\bar{u}_{NC,\,crt} = F_{0,\,NC,\,crt}\,\frac{T}{T_0}\,\frac{P_0}{P}\Big/(\pi(D/2)^2) \tag{41}$$

We obtain after rearranging Eqs. (39)–(41)

$$F_{0,\,NC,\,crt} = D_{CO_2,\,NC}\,\frac{L_{cal,\,crt}}{L^2_{D,\,Ar,\,crt}}\,\pi(D/2)^2\,\frac{T_0}{T}\,\frac{P}{P_0} \tag{42}$$

where

$L_{cal,\,crt}$ $\cong$ average($L_{cal,\,20-100\,ml\,min^{-1}}$), because it can be assumed that the total volume V_{tot} does not depend on the flow rate (Table 1 and Fig. 5) and = (12.81+12.53+11.76+13.54+13.69) / 5 = 12.9 cm; and

$L_{D,\,Ar,\,crt}$ $= \sqrt{D_{CO_2,\,Ar}\,\tau_{tot,\,critical}} = \sqrt{1.17\,cm^2\,s^{-1}\,\frac{1}{60}\,s} = 4.42\,cm$, (with $1/\tau_{tot,\,critical} = 3.6\,min^{-1}$, obtained from Fig. 9).

For helium, $D_{CO_2,\,He}$ is equal to 1.85 $cm^2\,s^{-1}$ for the above conditions what requires an increase in the total flow to about $F_0 = 116$ ml min^{-1} compared to

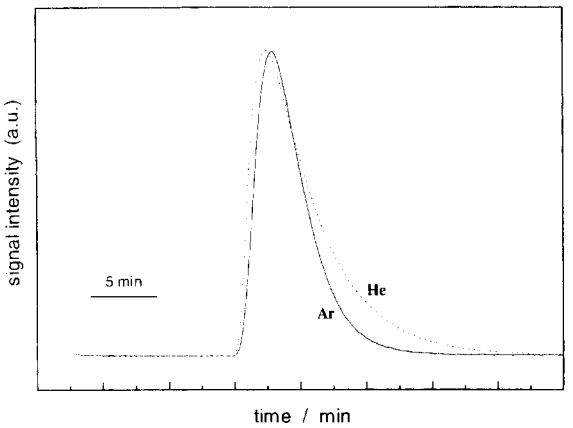

Fig. 10. MS curves obtained after injection of a 1 ml pulse of CO_2 into the carrier gas (Ar or He) flowing with a rate $F_0 = 20$ ml min^{-1}.

75 ml min^{-1} for argon. This ca. 1.5 higher flow causes a decrease in the CO_2 intensity recorded by the mass spectrometer. In the case of argon, a flow rate of 75 ml min^{-1} (NTP) is sufficient for a proper description of the thermoanalytical curve (DTG) from the MS curve, but this flow rate is obviously too low for helium. The higher diffusivity of CO_2 in He significantly changes the shape of the MS output curve what is especially visible at low flow rates. MS curves obtained by the injection of a 1 ml pulse of CO_2 into the stream of two different carrier gases: Ar and He ($F_0 = 20$ ml min^{-1}) are presented in Fig. 10. Due to the much higher molecular diffusion coefficient of CO_2 in helium than in argon, the mixed-flow zone in helium significantly increases. This fact indicates that in order to decrease the total gas flow through the thermoanalyser (what leads to an increase in the intensity of the MS curves) it is necessary to use a carrier gas such as argon in which the diffusivity of the evolved gas is low.

5. Conclusion

The decomposition of $CaCO_3$ has been used as a test reaction to investigate the interrelation between DTG and MS curves in a combined TA–MS. A model has been developed based on the separate consideration of three different zones in the system: the plug-flow, mixed-flow and dead zone. It takes into account the influence of convective and diffusional mass transfer which can result in significant deviation (time lag and shape of curves) between the measured DTG and MS curves. The model allows to quantify these deviations for particular experimental conditions (carrier gas-flow rate and diffusivity of evolved gas) and provides a criterion for finding the minimum carrier gas-flow rate at which the diffusional effects do not cause significant deviation between the DTG and MS curves. The criterion relates the total residence time to the characteristic time of the decomposition process. Generally, it can be stated that the higher the diffusivity of the evolving species in the carrier gas, the higher is the minimal required carrier gas-flow rate. Thus, the choice of the carrier gas strongly influences its minimal required flow rate and thereby the sensitivity of the mass spectrometric analysis.

6. Notations

β	heating rate (K min^{-1})
c	concentration (mol l^{-1})
d	parameter of the F-distribution (—)
D	internal diameter of the thermoanalytical chamber (cm)
$D_{CO_2,\,Ar}$	molecular diffusion coefficient of CO_2 in argon (cm^2 s^{-1})
$D_{CO_2,\,He}$	molecular diffusion coefficient of CO_2 in helium (cm^2 s^{-1})
$D_{CO_2,\,NC}$	molecular diffusion coefficient of CO_2 in the new carrier gas (cm^2 s^{-1})
DTG	derivative thermogravimetric curve (—)
δ	Dirac delta function, pulse (—)
Δt	interval of time (min)
ε	energy of molecular interaction in Lennard–Jones function (J)
f	residence-time distribution function (min^{-1})
f'	residence-time distribution of a Dirac delta function in a well-mixed reactor (min^{-1})
f_1	degree of freedom of the F-distribution (repeated experiments for experimental error determination) (—)

f_2	degree of freedom of the F-distribution (input and output signals) (—)
F_0	gas-flow rate of the carrier gas (NTP) ($cm^3\ min^{-1}$)
F	approximated formula of F-distribution for F-test (—)
g	normalised input signal, (obtained from the DTG-curve) (min^{-1})
h	normalised output signal, (obtained from the MS-curve) (min^{-1})
h'	$g(t-\tau_p)$ normalised input signal given by the thermoanalyser after plug-flow zone (min^{-1})
h''	$h(t+\tau_p)$ normalised output signal given by the mass spectrometer. Plug-flow zone removed (min^{-1})
H	height of the thermoanalyser chamber (cm)
i	i^{th} interval of time (—)
I	intensity of the signal measured by the mass spectrometer (A)
j	j^{th} interval of time (—)
J	amount of CO_2 measured by the mass spectrometer (A min)
k	Boltzmann constant 1.380658e−23 ($J\ K^{-1}$)
L_{cal}	calculated length of the thermoanalytical chamber without the dead region (cm)
L_D	length of the thermoanalytical chamber over which diffusion occurs (cm)
M	molecular weight ($g\ mol^{-1}$)
n	number of experimental points (—)
$\nu\ (=1/\Delta T)$	frequency of idealised pulses (Dirac delta functions) injected into the system (min^{-1})
NTP	normal temperature and pressure, 25°C and 1 atm
P	pressure (Pa)
Q	amount of CO_2 produced and measured by the thermoanalyser, weight loss of $CaCO_3$ (g)
R	signal given by the thermoanalyser, rate of weight loss by $CaCO_3$ ($g\ min^{-1}$)
RSS	$RSS(\tau_p, \tau_m)$ total residual sum of squares of the difference between the experimental and calculated values of the output signal h (min^{-2})
RSS_1	sum of residual squares between two (in order to consider the influence of the experimental errors) experiments performed under the same conditions (min^{-2})
RSS_2	sum of residual squares for one flow rate between the input and output signal given by the thermoanalyser and the mass spectrometer, respectively (min^{-2})
σ	'collision diameter' in Lennard–Jones function (Å)
t	reaction time (min)
T	temperature (K)
$\bar{T}$	average temperature for 50% conversion of $CaCO_3$ for five considered gas-flow rates F_0: 20, 40, 50, 80 and 100 ml min^{-1} (NTP) (K)
TG	thermogravimetric curve
t_N	characteristic time of the decomposition process, defined in Eq. (33) (min)
τ	residence time (min)
$\bar{u}$	average gas velocity in the thermoanalytical chamber ($cm\ s^{-1}$)
u_P	value of the standard normal distribution for P, f_1 and f_2 (—)
V	volume (cm^3)
Ω	'collision integral' for molecular diffusion in Lennard–Jones function (—)
z	function for the approximated F-distribution formula (—)

6.1. Subscripts

cal	calculated
crt	critical value given by the 'global criterion of the residence time'
d	dead zone
D	diffusion
exp	experimental
i	i^{th} interval of time Δt
in	input
j	j^{th} interval of time Δt
0	NTP, normal temperature and pressure
out	output
m	mixed flow
NC	new carrier gas under which the decomposition occurs

P	plug flow
tot	total

References

[1] O. Levenspiel, Chemical reaction engineering, 2nd edn., John Wiley and Sons, New York, London, 1972, p. 253.

[2] J.R. Welty, C.E. Wicks and R.E. Wilson, Fundamentals of Momentum, Heat, and Mass Transfer, 3rd edn., John Wiley and Sons, New York, London, 1984, p. 487.

[3] M. Baerns, H. Hofmann and A. Renken, Chemische Reaktionstechnik, Georg Thieme Verlag, Stuttgart, New York, 1987, p. 68.

[4] D. Rasch, G. Herrendörfer, J. Bock and K. Busch, Verfahrensbibliothek-Versuchsplanung und -Auswertung, VEB Deutscher Verlag Landwirtschaftverlag, Berlin, 1981, p. 1105.